Research in Astron. Astrophys. **2011** Vol. **11** No. **4**, 369–390
http://www.raa-journal.org *http://www.iop.org/journals/raa*

Research in Astronomy and Astrophysics

INVITED REVIEWS

The astrophysical gravitational wave stochastic background

Tania Regimbau

UMR ARTEMIS, CNRS, University of Nice Sophia-Antipolis, Observatoire de la Côte d'Azur, BP 4229, 06304, Nice Cedex 4, France; *regimbau@oca.eu*

Received 2010 February 14; accepted 2010 September 7

Abstract A stochastic background of gravitational waves with astrophysical origins may have resulted from the superposition of a large number of unresolved sources since the beginning of stellar activity. Its detection would put very strong constraints on the physical properties of compact objects, the initial mass function and star formation history. On the other hand, it could be a 'noise' that would mask the stochastic background of its cosmological origin. We review the main astrophysical processes which are able to produce a stochastic background and discuss how they may differ from the primordial contribution in terms of statistical properties. Current detection methods are also presented.

Key words: gravitational waves — stochastic background: neutron stars — black holes

1 INTRODUCTION

Gravitational wave (GW) astronomy will enable a new window to the Universe to be opened: not only does one expect to discover a set of new exotic sources, but also to travel back in time, toward the very early stages of the evolution of the Universe. According to various cosmological scenarios, we are bathed in a stochastic background of gravitational waves, the memory of the first instant of the Universe, up to the limits of the Plank era and the Big Bang (Grishchuk et al. 2001). Proposed theoretical models include the amplification of vacuum fluctuations during inflation (Grishchuk 1974, 1993; Starobinskiĭ 1979), pre-Big Bang models (Gasperini & Veneziano 1993, 2003; Buonanno et al. 1997), cosmic strings (Vilenkin & Shellard 2000) and phase transitions (Caprini 2010) (see Maggiore 2000 for a general review and references therein). In addition to this cosmological gravitational background (CGB), an astrophysical contribution (AGB) may have resulted from the superposition of a large number of unresolved sources since the beginning of stellar activity, which can be either short lived burst sources, such as core collapses to neutron stars (Blair & Ju 1996; Coward et al. 2001, 2002; Howell et al. 2004; Buonanno et al. 2005; Marassi et al. 2009; Zhu, Howell & Blair 2010) or black holes (Ferrari et al. 1999a; de Araujo et al. 2000, 2002a,b, 2004), oscillation modes (Owen et al. 1998; Ferrari et al. 1999b; Marassi et al. 2009; Zhu, Howell & Blair 2010), final stage of compact binary mergers (Regimbau & de Freitas Pacheco 2006b; Regimbau 2007), or periodic long live sources, typically pulsars (Regimbau & de Freitas Pacheco 2001a, 2006a), the early inspiral phase of compact binaries (Ignatiev et al. 2001; Schneider et al. 2001; Farmer & Phinney 2002; Cooray 2004) or captures by supermassive black holes (Barack & Cutler 2004; Schnittman et al. 2006), whose frequency is expected to evolve very slowly compared to the observation time. The

nature of the AGB may differ from its cosmological counterpart, and is expected to be stationary, unpolarized, Gaussian and isotropic, by analogy with the cosmic microwave background (CMB). On one hand, the distribution of galaxies with distances up to 100 Mpc is not isotropic, but rather is strongly concentrated in the direction of the VIRGO cluster and the Great Attractor; on the other hand, depending on whether the time interval between events is short compared to the duration of a single event, the integrated signal may result in continuous, popcorn noise or shot noise background (Coward & Regimbau 2006). The optimal strategy to search for a Gaussian (or continuous) stochastic background is to cross correlate measurements from multiple detectors, which can be either resonant antennas such as the cryogenic bars AURIGA, NAUTILUS, EXPLORER, ALLEGRO or NIOBE (Amaldi et al. 1990; Cerdonio et al. 1997; Pallottino 1997; Mauceli et al. 1996; Blair et al. 1995), laser interferometers such as LIGO, VIRGO, GEO600, TAMA300/LCGT and the third generation Einstein Telescope (Abramovici et al. 1992; Bradaschia et al. 1990; Hough 1992; Kuroda et al. 2006) on earth or LISA in space (Bender & the LISA Study Team 1998), or natural detectors such as millisecond pulsars of the Parkes Pulsar Timing Array (PPTA) (Jenet et al. 2005; Manchester 2006). Space and terrestrial detectors will be complementary in the $10^{-5} - 10^{4}$ Hz band, while the PPTA is expected to detect GWs at nHz frequencies. Over the last decade, the first generation of terrestrial detectors has been built, commissioned and is running in scientific mode at (or close to) their design sensitivities, providing the opportunity to do joint data analysis.

This paper gives an overview of the main features of the AGBs, from modeling to detection, and discusses how their statistical properties may differ from those of the cosmological background. In Section 2, we review the spectral and statistical properties of astrophysical backgrounds, in Section 3 we introduce the actual detection method to search for a stochastic background in a network of detectors, in Section 4 we review the most popular predictions of the cosmological background, in Section 5 we describe models of AGB and in Section 6 we discuss the current observational results and future prospects.

2 THE CHARACTERISTICS OF THE SPECTRUM

The spectrum of the gravitational stochastic background is usually characterized by the dimensionless parameter (Allen & Romano 1999)

$$\Omega_{\rm gw}(\nu_{\rm o}) = \frac{1}{\rho_{\rm c}} \frac{d\rho_{\rm gw}}{d\ln \nu_{\rm o}}, \tag{1}$$

where $\rho_{\rm gw}$ is the gravitational energy density, $\nu_{\rm o}$ the frequency in the observer frame and $\rho_{\rm c} = \frac{3H_0^2}{8\pi G}$ the critical energy density needed to make the present Universe flat. Experimentalists may prefer to work with the spectral energy density,

$$S_h(\nu_{\rm o}) = \frac{3H_0^2}{4\pi^2} \frac{1}{\nu_{\rm o}^3} \Omega_{\rm gw}(\nu_{\rm o}), \tag{2}$$

which is directly comparable to the detector sensitivity.

For a stochastic background of astrophysical origin, the energy density parameter is given by (Ferrari et al. 1999a)

$$\Omega_{\rm gw} = \frac{1}{\rho_{\rm c} c^3} \nu_{\rm o} F_{\nu_{\rm o}}, \tag{3}$$

where the integrated flux at the observed frequency $\nu_{\rm o}$ is defined as

$$F_{\nu_{\rm o}} = \int p(\theta) f_{\nu_{\rm o}}(\theta, \nu_{\rm o}) \frac{dR^o(\theta, z)}{dz} d\theta dz, \tag{4}$$

where $p(\theta)$ is the probability distribution of the source parameters θ. The first factor in the integral is the fluence of a source located at redshift z

$$f_{\nu_o}(\theta, \nu_o) = \frac{1}{4\pi(1+z)r(z)^2} \frac{dE_{gw}}{d\nu}(\theta, \nu_o), \tag{5}$$

where $r(z)$ is the proper distance, which depends on the adopted cosmology, $\frac{dE_{gw}}{d\nu}(\theta, \nu_o)$ the gravitational spectral energy emitted and $\nu = \nu_o(1+z)$ the frequency in the source frame. The second factor is the number of sources in the interval $\theta - \theta + d\theta$, per unit of time in the observer frame and per redshift interval, which is given by

$$\frac{dR^o(\theta, z)}{dz} = \dot{\rho}^o(\theta, z) \frac{dV}{dz}(z), \tag{6}$$

where $\dot{\rho}^o(\theta, z)$ is the event rate in Mpc^{-3} yr^{-1} and $\frac{dV}{dz}(z)$ the comoving volume element.

Combining the expressions above, one obtains for the density parameter

$$\Omega_{gw}(\nu_o) = \frac{8\pi G}{3c^2 H_0^3} \nu_o \int d\theta p(\theta) \int_{z_{inf}}^{z_{sup}} dz \frac{\dot{\rho}^o(\theta, z)}{(1+z)E(\Omega, z)} \frac{dE_{gw}(\nu_o)}{d\nu}(\theta, \nu_o). \tag{7}$$

Replacing the constants by their usual values we get

$$\Omega_{gw}(\nu_o) = 5.7 \times 10^{-56} \left(\frac{0.7}{h_0}\right)^2 \nu_o \int d\theta p(\theta) \int_{z_{inf}}^{z_{sup}} dz \frac{\dot{\rho}^o(z)}{(1+z)E(\Omega, z)} \frac{dE_{gw}(\nu)}{d\nu}, \tag{8}$$

where $\dot{\rho}^o$ is given for $h_0 = 0.7$. The limits of the integral over z depend on both the emission frequency range in the source frame, and the redshift interval, where the source can be located as

$$z_{sup}(\theta, \nu_o) = \begin{cases} z_{max} & \text{if } \nu_o < \frac{\nu_{max}}{(1+z_{max})}, \\ \frac{\nu_{max}}{\nu_o} - 1 & \text{otherwise}, \end{cases} \tag{9}$$

and

$$z_{min}(\theta, \nu_o) = \begin{cases} z_{min} & \text{if } \nu_o > \frac{\nu_{min}}{(1+z_{min})}, \\ \frac{\nu_{min}}{\nu_o} - 1 & \text{otherwise}. \end{cases} \tag{10}$$

Consequently, the shape of the spectrum of any astrophysical background is characterized by a cutoff at the maximal emission frequency and a maximum at a frequency which depends on the shape of both the redshift distribution and the spectral energy density.

For most of the models presented in Section 5, the event rate per unit of redshift can be derived directly from the cosmic star formation rate. In the simple case, where the gravitational emission occurs shortly after the birth of the progenitor, it is given by

$$\dot{\rho}^o(\theta, z) = \lambda(\theta, z) \frac{\dot{\rho}_*(z)}{1+z}, \tag{11}$$

where λ is the mass fraction converted into the progenitors in $M_\odot^{-1}$, which depends on the initial mass function, $\frac{dV}{dz}$ the element of comoving volume and $\dot{\rho}_*(z)$ the cosmic star formation rate (SFR) in $M_\odot$ Mpc^{-3} yr^{-1}. The $(1+z)$ factor in the denominator corrects for the time dilatation due to cosmic expansion.

Observations of star forming galaxies with large telescopes such as the Keck or the Hubble Space Telescope have extended our view of the Universe up to redshifts $z \sim 5-6$, by tracing the evolution with cosmic time of the galaxy luminosity density. The main uncertainty comes from dust extinction, which spreads the UV luminosity into the far IR. Madau et al. (1998) derived an expression that matches most of the measurements in the U-V continuum and Hα, up to $z \sim 4$, and that includes an

extinction correction of A_{1500}=1.2 mag. The SFR is expected to increase rapidly between $z \sim 0-1$, peak around $z \sim 1.7$ and smoothly decrease at large redshifts. After $z \sim 2$, the behavior must be regarded as tentative, due to the large uncertainties in the estimates of the U-V luminosity from the Lyman break galaxies in the Hubble Deep Field. Steidel et al. (1999) proposed another scenario where the SFR remains constant after $z \sim 2$. Other studies suggested there may even be an increase in the SFR, claiming that it could have been severely underestimated due to a large amount of dust extinction (Blain et al. 1999). However, the hypothesis of a gentle decline at high redshifts seems to be favored by new measurements of the galaxy luminosity function in the UV (SDSS, GALEX, COMBO17) and FIR wavelengths (Spitzer Space Telescope), which allowed researchers to refine the previous models of star formation history, up to redshift $z \sim 6$, with tight constraints at redshifts $z < 1$. In a recent work, Hopkins & Beacom (2006) used the Super Kamiokande limit on the electron antineutrino flux from past core-collapse supernovae to derive parametric fits of the form of Cole et al. (2001). Investigating the effect of the initial mass function (IMF) on the normalization of the SFR, they showed that top heavy IMFs are preferred to the traditional Salpeter IMF (Salpeter 1955), and the fits are optimized for IMFs of the form

$$\xi(m) \propto \begin{cases} (\frac{m}{m_0})^{-1.5} & \text{for } 0.1 < m < m_0 \\ (\frac{m}{m_0})^{-\gamma} & \text{for } m_0 < m < 100 \end{cases} \tag{12}$$

with a turnover below $m_0 = 0.5\,M_\odot$, normalized within the mass interval $0.1 - 100\,M_\odot$ such as $\int m\xi(m)dm = 1$, and with $\gamma = 2.35$ (A modified Salpeter). Fardal et al. (2007) used a different set of measurements and different dust extinction corrections and found an SFR similar to that of Hopkins & Beacom (2006) up to $z \sim 1$, but which decreases slightly at higher redshifts. Wilkins et al. (2008) used measurements of the stellar mass density and derived an SFR equivalent to that of Hopkins & Beacom (2006) and Fardal et al. (2007) for redshifts smaller than $z \sim 0.7$, but again is lower at higher redshifts. Finally, Nagamine et al. (2006) derived a model from the fossil record of star formation in nearby galaxies. It is probably underestimated at small redshifts, and is constant at high redshifts due to the contribution of elliptical galaxies. Note that at present there is a discrepancy between the "instantaneous" SFR, measured from the emission of young stars in star forming regions, and the SFR as determined from extragalactic background light. This could have an important impact on the contribution to the confusion background for sources from $z > 2$. However, it should not noticeably affect the results, since sources beyond $z \sim 2$ are too weak to contribute significantly to the integrated signal.

Figure 1 compares the four prior models described above, calculated for the flat Einstein-de Sitter 737 cosmology, with $\Omega_m = 0.3$, $\Omega_\Lambda = 0.7$ and Hubble parameter $H_0 = 70\,\mathrm{km\ s^{-1}\ Mpc^{-1}}$ (Rao et al. 2006), corresponding to the so-called concordant model derived from observations of distant type Ia supernovae (Perlmutter et al. 1999) and the power spectra of the cosmic microwave background fluctuations (Spergel et al. 2003).

Besides the spectral properties, it is important to study the nature of the background. In the case of short-lived signals, they may show very different statistical behavior depending on the ratio between the duration of the events and the time interval between successive events, with duty cycle

$$\Delta(z) = \int_0^z \bar{\tau}(1+z')\frac{dR^o(z')}{dz'}dz', \tag{13}$$

which is also the average number of events present at the detector at a given observation time.

Continuous: the number of sources is large enough for the time interval between events to be small compared to the duration of a single event. The waveforms overlap to create a continuous background and, due to the central limit theorem, such backgrounds obey Gaussian statistical properties. They are completely determined by their spectral properties and could be detected by data analysis methods in the frequency domain such as the standard cross correlation statistic (Allen & Romano 1999).

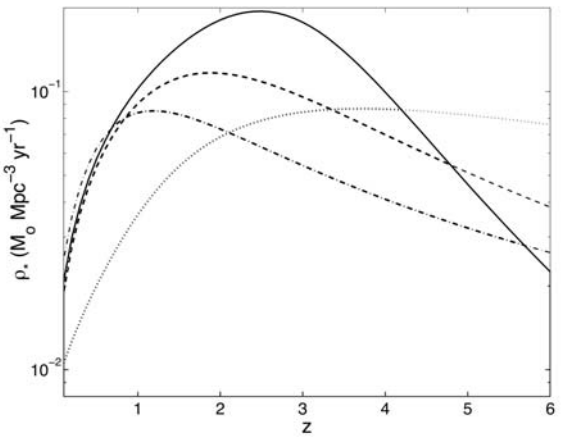

Fig. 1 Cosmic star formation rates (in $M_\odot\,\mathrm{Mpc}^{-3}\,\mathrm{yr}^{-1}$) used in this paper: Hopkins & Beacom (2006) (*solid line*), Fardal et al. (2007) (*dashed line*), Wilkins et al. (2008) (*dot-dashed line*), and the fossil model of Nagamine et al. (2006) (*dotted line*). As discussed in the text, these rates are largely the same up to $z \sim 1$, but show important differences at higher redshift.

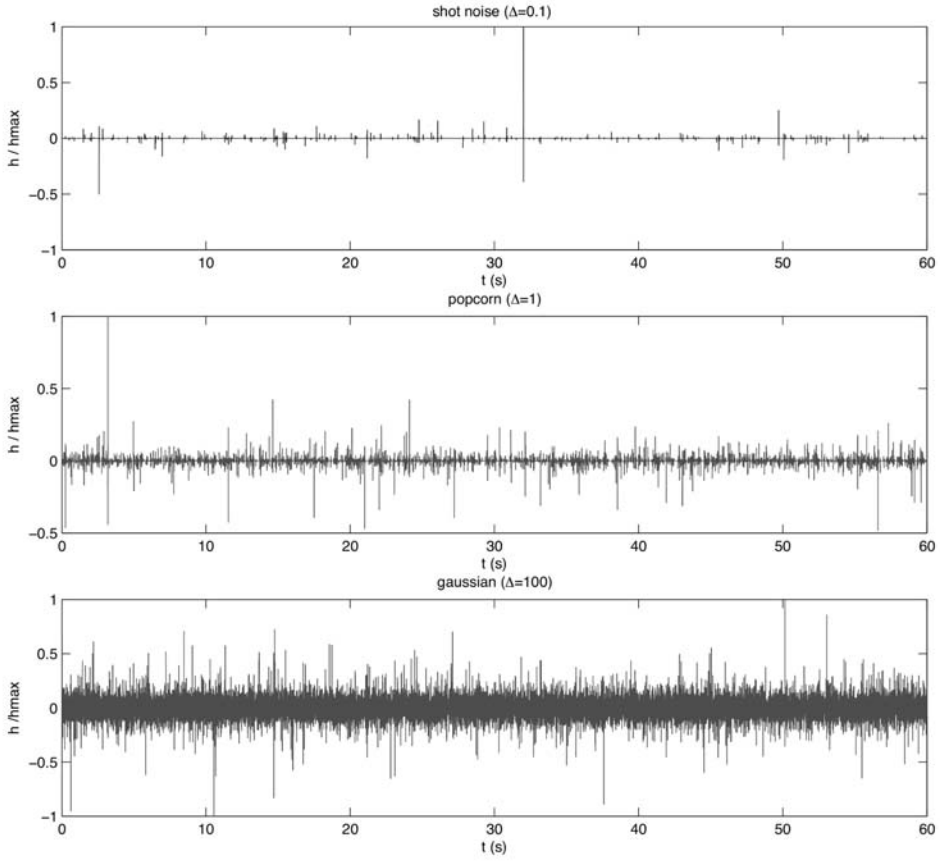

Fig. 2 Time series corresponding to shot noise, popcorn and Gaussian regimes.

Shot noise: the number of sources is small enough for the time interval between events to be long compared to the duration of a single event. The waveforms are separated by long stretches of silence and the closest sources may be detected by data analysis techniques in the time domain (or the time frequency domain) such as matched filtering (Arnaud et al. 1999; Pradier et al. 2001).

Popcorn: an interesting intermediate case arises when the time interval between events has the same order of the duration as a single event. These signals, which sound like crackling popcorn, are known as "popcorn noise." The waveforms may overlap but the statistical properties are not Gaussian anymore and the amplitude on the detector at a given time is unpredictable. Promising data analysis strategies have been investigated in the last few years, such as the Maximum Likelihood statistic, an extension of the cross correlation statistic in the time domain (Drasco & Flanagan 2003) or methods based on the Probability Event Horizon concept (Coward & Burman 2005), which describes the evolution of the cumulated signal throughout the Universe, as a function of the observation time. Time series corresponding to the three different regimes are illustrated in Figure 2.

3 DETECTION

The optimal strategy to search for a Gaussian (or continuous) stochastic background, which can be confounded with the intrinsic background noise of the instrument, is to cross correlate measurements from multiple detectors. In this section, we give a brief overview of the standard data analysis technique currently used for terrestrial interferometers.

When the background is assumed to be isotropic, unpolarized and stationary, the cross correlation product is given by Allen & Romano (1999)

$$Y = \int_{-\infty}^{\infty} \tilde{s_1}^*(f)\tilde{Q}(f)\tilde{s_2}(f)df, \tag{14}$$

where

$$\tilde{Q}(f) \propto \frac{\Gamma(f)\Omega_{\rm gw}(f)}{f^3 P_1(f)P_2(f)} \tag{15}$$

is a filter that maximizes the signal to noise ratio (S/R). In the above equation, $P_1(f)$ and $P_2(f)$ are the power spectral noise densities of the two detectors and Γ is the non-normalized overlap reduction function, characterizing the loss of sensitivity due to the separation and the relative orientation of the detectors (Fig. 3). The optimized S/N ratio for an integration time T is given by Allen (1997)

$$\left(\frac{\rm S}{\rm N}\right)^2 = \frac{9H_0^4}{8\pi^4} T \int_0^{\infty} df \frac{\Gamma^2(f)\Omega_{\rm gw}^2(f)}{f^6 P_1(f)P_2(f)}. \tag{16}$$

In the literature, the sensitivity of a pair of detectors is usually given in terms of the minimum detectable amplitude corresponding to $\Omega_{\rm gw}$ equal to a constant (hereafter a flat spectrum) (Allen & Romano 1999):

$$\Omega_{\rm min} = \frac{4\pi^2}{3H_0^2\sqrt{T}} \left[{\rm erfc}^{-1}(2\beta) - {\rm erfc}^{-1}(2\alpha)\right] \left[\int_0^{\infty} df \frac{\Gamma^2(f)}{f^6 P_1(f)P_2(f)}\right]^{-1/2}. \tag{17}$$

The expected minimum detectable amplitudes for the main terrestrial interferometer pairs, at design sensitivity (Fig. 4), and after one year of integration, are given in Table 1, for a detection rate of $\alpha = 90\%$ and a false alarm rate of $\beta = 10\%$.

$\Omega_{\rm min}$ is on the order of $10^{-6} - 10^{-5}$ for the first generation of interferometers combined as LIGO/LIGO and LIGO/Virgo. Their advanced counterparts will permit an increase of two or even three orders of magnitude in sensitivity ($\Omega_{\rm min} \sim 10^{-9} - 10^{-8}$). The pair formed by the co-located and co-aligned LIGO Hanford detectors, for which the overlap reduction function is equal to one,

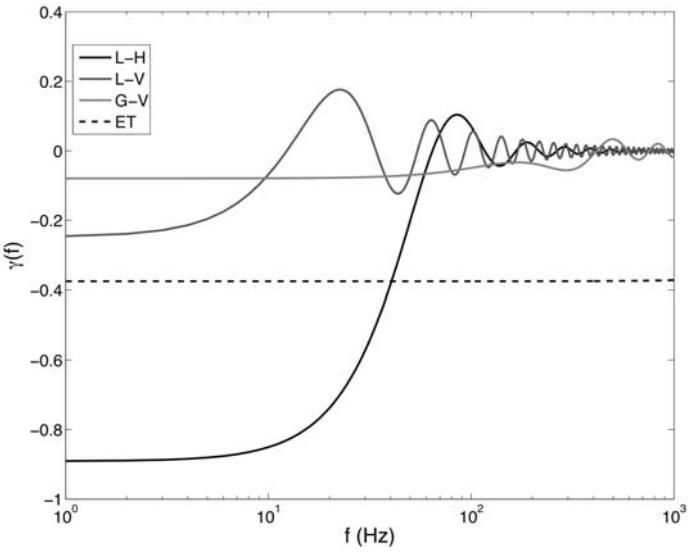

Fig. 3 Overlap reduction function for the most promising detector pairs. L stands for LIGO Livingston and H for LIGO Hanford, V for Virgo, G for GEO600 and ET for the planned Einstein Telescope in the triangular configuration.

is potentially one order of magnitude more sensitive than the Hanford/Livingston pair, provided that instrumental and environmental noises can be removed.

In Table 2, we show the evolution of the upper limit obtained with the LIGO detectors in a narrow band around 100 Hz, which corresponds to $\Omega_{\rm gw}$ equaling a constant at all frequencies. In Table 3, the latest published LIGO upper limit is compared to observational limits already achieved with resonant bar experiments at about 900 Hz and pulsar timing observations at nHz frequencies.

Table 1 Expected $\Omega_{\rm min}$ for the main detector pairs, corresponding to a flat background spectrum, one year of integration over the full frequency band, a detection rate of $\alpha = 90\%$ and a false alarm rate of $\beta = 10\%$. LHO and LLO stand for LIGO Hanford Observatory and LIGO Livingston Observatory respectively, and ET stands for the planned Einstein Telescope in the triangular configuration (Flanagan 1993).

	LHO-LHO	LHO-LLO	LLO-VIRGO	VIRGO-GEO
Initial	4×10^{-7}	3×10^{-6}	6×10^{-6}	2×10^{-5}
Advanced	6×10^{-9}	1×10^{-9}		
ET	5×10^{-12}			

An extension of the cross-correlation method to non-isotropic contributions has been investigated by Allen & Ottewill (1997); Cornish (2001); Ballmer (2006) and Mitra et al. (2008). The basic idea is to use multiple detector pairs to create maps of anisotropy of the GW background, similar to a radiometer of GWs.

4 RELIC STOCHASTIC BACKGROUND

Mechanisms able to generate stochastic backgrounds of GWs in the very early stages of the Universe have been investigated intensively in the past decades (Fig. 5). Their detection would have a pro-

Table 2 Evolution of the LIGO 90% Bayesian upper limit of a frequency independent $\Omega_{\rm gw}$.

Run	Frequency band (Hz)	Upper limit	Reference
S1	$40-314$	23	Abbott et al. (2004)
S3	$69-156$	8.4×10^{-4}	Abbott et al. (2005)
S4	$51-150$	6.5×10^{-5}	Abbott et al. (2007)
S5	$40-170$	5.9×10^{-6}	Abbott et al. (2009)

Table 3 Best published direct upper limits of a frequency independent $\Omega_{\rm gw}$ derived from correlation, for different types of experiments.

Type of detectors	Experiment	Frequency (Hz)	Upper limit	Reference
Room temp. resonant bars	Glasgow	985	6125	Hough et al. (1975)
Cryogenic resonant bar	Explorer+Nautilus	907	120	Astone et al. (1999)
Pulsar timing	Parkes	10^{-8}	4×10^{-8}	Jenet et al. (2005)

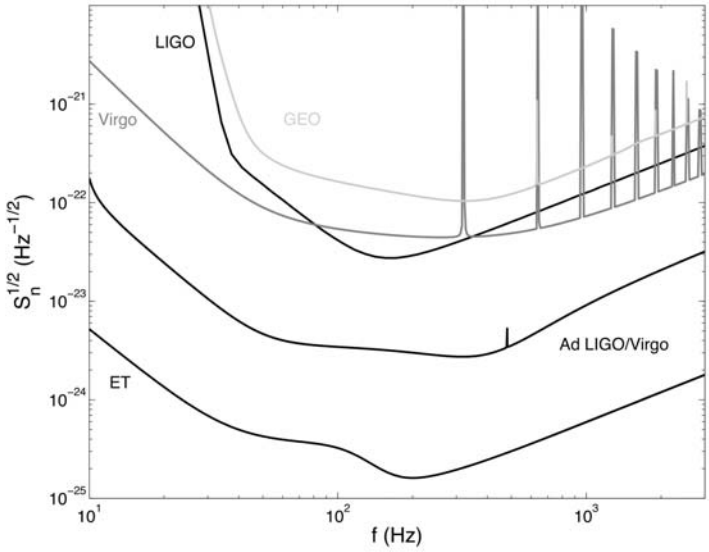

Fig. 4 Designed sensitivities of the main first generation interferometers, compared to the planned sensitivities of advanced detectors (LIGO or Virgo) and third generation detectors (Einstein Telescope).

found impact on our understanding of near Big Bang cosmology and high energy physics, providing a unique way to explore the Universe a fraction of a second after the Big Bang, after gravitons decoupled from the primordial plasma. It is not the purpose of this article to develop in detail all the different models of cosmological stochastic background present in the literature, as our main interest is the astrophysical background, but for comparison purpose, we give a rapid overview of some popular predictions that could be masked by the astrophysical background in this section. We refer interested readers to very nice review papers by Allen (1997); Maggiore (2000) and Buonanno (2003).

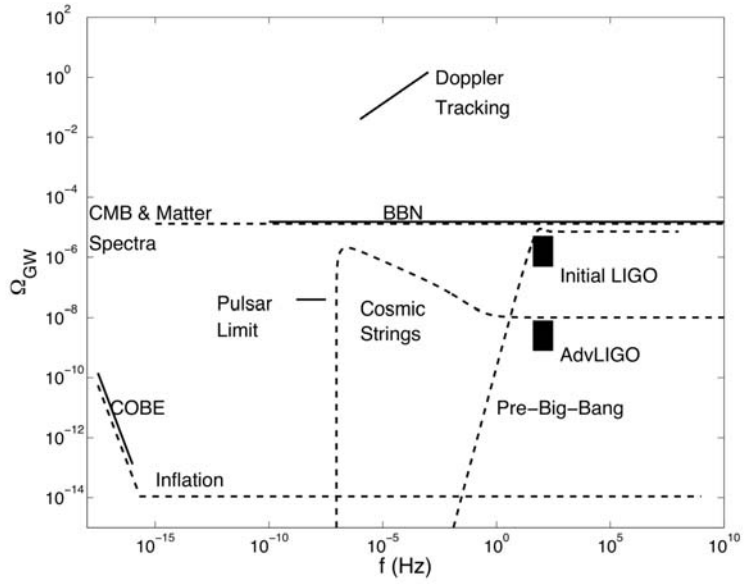

Fig. 5 Theoretical predictions of the cosmological stochastic background and observational bounds. The cosmic string plot corresponds to $p = 0.1$, $\varepsilon = 7 \times 10^{-5}$, and $G\mu = 10^{-8}$. This figure was kindly provided by Vuk Mandic.

In this section, unless it is mentioned otherwise, the Hubble parameter is assumed to be $H_0 = 70\,\mathrm{km\,s^{-1}\,Mpc^{-1}}$.

4.1 Amplification of Vacuum Fluctuations

Amplifications of vacuum fluctuations at the transitions between the de Sitter, radiation dominated (RD) and matter dominated (MD) eras, first discussed by Grishchuk (1974, 1993) and Starobinskiĭ (1979), are expected to produce a GW background whose spectrum and amplitude depend strongly on the fluctuation power spectrum developed during the early inflationary period. The standard de Sitter inflation predicts a spectrum that decreases as $1/f^2$ in the range $3\times10^{-18}-10^{-16}$ Hz and then remains constant in a very large band up to MHz frequencies. In the low frequency region, modes amplified during inflation at both the de Sitter-RD and RD-MD transitions contribute. The turnover between the two phases corresponds to the limit at which only the modes amplified during the de Sitter-RD transition can be observed. The COBE experiment, which has the same $1/f^2$ behavior in the low frequency region, provides an upper bound of $\Omega_{\rm gw} \sim 9\times10^{-14}$ (Maggiore 2000; Buonanno 2003) for the flat region. Actually, a GW background larger than $\Omega_{\rm gw} \sim 7\times10^{-10}(\frac{10^{-18}}{f})^2$ at frequencies between $3\times10^{-18}-10^{-16}$ Hz would have produced stochastic frequency redshifts through Sachs-Wolfe effects, which would have resulted in temperature fluctuations larger than those measured for the cosmic microwave background. In the more realistic scenario of "slow roll down" inflation, the inflation field rolls toward the minimum of its potential, producing an acceleration of the expansion. The Hubble parameter is not constant as in the standard scenario, but decreases monotonically during the period of inflation. GWs are produced by fluctuations that go out of the Hubble radius during inflation, and re-enter in the radiation era. The resulting spectrum is not flat like that of the de Sitter inflation but rather has an f^{n_T} dependency, where $n_T < 0$ and $|n_T| \ll 1$. The

spectral index can be expressed in terms of the scalar and tensorial contributions to the quadrupole cosmic microwave background (CMB) anisotropy as $n_T = -T/7S$ (Maggiore 2000). The most optimistic predictions for a detection with LISA at $f \sim 10^{-4}$, corresponding to $n_T = 0.175$, give an amplitude $\Omega_{\rm gw} \sim 10^{-15}$, but n_T could be much smaller, on the order of 10^{-3} (Maggiore 2000). In a recent paper, Tong & Zhang (2009) studied the effect of a running spectral index α_t on the GW spectrum and found that $\alpha_t > 0$ could enhance the signal significantly, especially at high frequencies.

A more interesting case arises from pre-big-bang scenarios in string cosmology (Gasperini & Veneziano 1993, 2003). According to these models, the standard RD and MD eras were preceded by phases in which the Universe was first large and shrinking (inflaton phase) and then characterized by a high curvature (stingy phase). The GW spectrum produced at the transition between the stingy phase and the RD era is described as $\Omega_{\rm gw} \sim f^3$ for $f < f_s$ and $\Omega_{\rm gw} \sim f^{3-2\mu}$ for $f_s < f < f_1$ (Buonanno et al. 1997; Mandic & Buonanno 2006). The turnover frequency is essentially unconstrained; $\mu < 1.5$ reflects the evolution of the Universe during the 'stingy' phase and the cutoff frequency f_1, which depends on string related parameters, has a typical value of 4.3×10^{10} Hz. An upper limit on $\Omega_{\rm gw}$ is imposed by the Big Bang Nucleosynthesis (BBN) bound down to 10^{-10} Hz, corresponding to the horizon size at the time of BBN. Actually, if the amount of total energy carried by GWs, $\int \Omega_{\rm gw} d(\ln f)$, at the time of nucleosynthesis was larger than $1.1 \times 10^{-5}(N_\nu - 3)$, where N_ν is the effective relative number of species at the time of BBN, it would have resulted in a particle production rate too large compared to the expansion of the Universe to account for the primordial abundances of the light elements ^{2}H, ^{2}He, ^{4}He and ^{7}Li. Measurements of the light element abundances combined with the WMAP data give $N_\nu < 4.4$ (Cyburt et al. 2005), which translates into $\Omega_{\rm gw} < 1.5 \times 10^{-5}$. Recent measurements of the CMB anisotropy spectrum, galaxy power spectrum and of the Lyman-α forest give a bound with a similar amplitude which extends down to 10^{-15} Hz, corresponding to the horizon size at the time of CMB decoupling (Smith et al. 2006).

4.2 Cosmic Strings

Cosmic strings, formed as linear topological defects during symmetry breaking phase transitions or in string theory inspired inflation scenarios, may emit GWs by oscillating relativistically and shrinking in size (Buonanno 2003). CMB observations are not consistent with the most promising scenario of very large mass-per-unit-length strings, acting as initial seeds for the formation of large-scale structures at the GUT scale symmetry break, but strings of lower energy scale may still contribute to the CGB. Also, in models with a non-vanishing cosmological constant, this approach can still be a viable option (Avelino et al. 1998; Battye et al. 1998). The spectrum is expected to peak around the frequency $f \sim 10^{-12}$ Hz and become almost flat in a large frequency band from 10^{-8} to 10^{10} Hz, where the amplitude can reach $\Omega_{\rm gw} \sim 10^{-9} - 10^{-8}$, according to numerical simulations of a network of cosmic strings with $G\mu < 10^{-6}$ (Buonanno 2003). At the present time, the most stringent constraint is given by pulsar timing observations. When passing between Earth and pulsars, GWs may cause fluctuations in the arrival time of the pulses. Observations of PSR B1805+09 (Kaspi et al. 1994; Lommen et al. 2003), a very stable narrow profile millisecond pulsar, with the Arecibo and Green Bank radio telescopes for over 17 yr, give an upper limit of $\Omega_{\rm gw} \sim 1.2 \times 10^{-9}$ at the frequency $f = \frac{1}{T_{\rm obs}} = 1.86 \times 10^{-9}$ nHz, and combining the timings of seven pulsars (Jenet et al. 2005) placed a lower bound of $\Omega_{\rm gw} \sim 4 \times 10^{-8}$. The Parkes Pulsar Timing Array project (Manchester 2006) which is expected to reach $\Omega_{\rm gw} \sim 2 \times 10^{-10}$, by monitoring twenty pulsars for five years, may be our best hope to detect cosmic strings in the near future.

In a recent work, Damour & Vilenkin (2000, 2001, 2005) and Siemens et al. (2007) considered the stochastic background created by cusps of oscillating cosmic superstring loops at the end of Brane inflation. The amplitude and shape of the GW spectrum is determined by three parameters (Damour & Vilenkin 2005): the string tension μ, the reconnection probability p, typically in the

range $10^{-3}-1$ and ε, the typical size of the closed loops produced in the string network. In particular, μ and ε determine the lowest frequency at which a string loop can emit GWs. The GW spectrum is characterized by a decrease at the lowest frequencies, followed by a flat region. Assuming $p = 5 \times 10^{-3}$, $G\mu = 10^{-7}$ and $\varepsilon = 10^{-7}$, Siemens et al. (2007) obtained a spectrum that avoids the low frequency bound due to CMB or pulsar timing measurements but still remains in the sensitivity band of space or ground based detectors. Let us mention that according to Damour & Vilenkin (2000, 2001, 2005), occasional strong beams of GWs could be produced at cusps, forming popcorn-like noise on top of the Gaussian contribution.

4.3 Phase Transitions

At the early stages of its evolution, the Universe may have undergone several episodes of phase transition, in which the symmetry of fundamental particle-physics interactions spontaneously broke. This may occur for instance at the QCD (150 MeV) and electroweak scales (100 GeV) or even earlier, at the grand unified scale (see Maggiore 2000 and references therein). The Standard Model predicts a rather smooth crossover, but in its supersymmetric extensions, the transition from a metastable phase (the false vacuum) to the state of broken symmetry (the true vacuum) can be first order, and a large amount of GWs could be produced when bubbles of the new phase are nucleated, grow and as they become more numerous, collide at very high velocities. The GW spectrum reaches a maximum of $\Omega_{\rm gw} \sim 10^{-6}(\frac{H_*}{\beta})^2(\frac{100}{N_*})^{1/3}$ at $f_{\rm max} \sim 3 \times (\frac{\beta}{H_*})(\frac{N_*}{100})^{1/6}T_*$, where $\Gamma = \Gamma_0 e^{-\beta t}$ is the nucleation rate of bubbles, T_* is the temperature in GeV of the phase transition, H_* the relevant Hubble parameter and N_* the number of relativistic degrees of freedom. In particular, a phase transition at the electroweak scale could give a detectable signal of $\Omega_{\rm gw} \sim 10^{-9}$ at the mHz frequency, where LISA is the most sensitive. Besides the collision of the broken phase bubbles, other processes are expected to produce gravitational waves, such as the magnetohydrodynamical turbulence in the plasma stirred by the bubble collisions, and the magnetic fields amplified by the magnetohydrodynamical turbulence (Caprini 2010).

5 SOURCES OF ASTROPHYSICAL BACKGROUNDS

Many examples of astrophysical backgrounds can be found in the literature. However, a direct comparison between the different models is made difficult by the fact that they often use different cosmologies, SFRs, IMFs, or mass ranges for neutron star (NS) or black hole (BH) progenitors. In this section, we review some of the most promising predictions, since it is impossible to cover all the literature on the subject here (Fig. 6).

5.1 Binary Neutron Stars

Double neutron star coalescences, which may radiate about 10^{53} erg in the last seconds of their inspiral trajectory, up to $1.4 - 1.6$ kHz, may be the most important contribution in the frequency range of ground based detectors (Regimbau & de Freitas Pacheco 2006b; Regimbau & Mandic 2008).

The coalescence rate per comoving volume $\dot{\rho}^{\rm o}$ in Equation (8) results from the convolution of the formation rate of the progenitors with the probability distribution P of the delay $t_{\rm d}$ between the formation of the progenitors and the coalescence

$$\dot{\rho}_{\rm c}^{o}(z) \propto \int \frac{\dot{\rho}_*(z_f)}{(1+z_f)} P(t_{\rm d})\, dt_{\rm d}, \tag{18}$$

where z is the redshift at the time of the coalescence and z_f is the redshift at the time of formation of the binary. Population synthesis models (Piran 1992; Tutukov & Yungelson 1994; Lipunov et al.

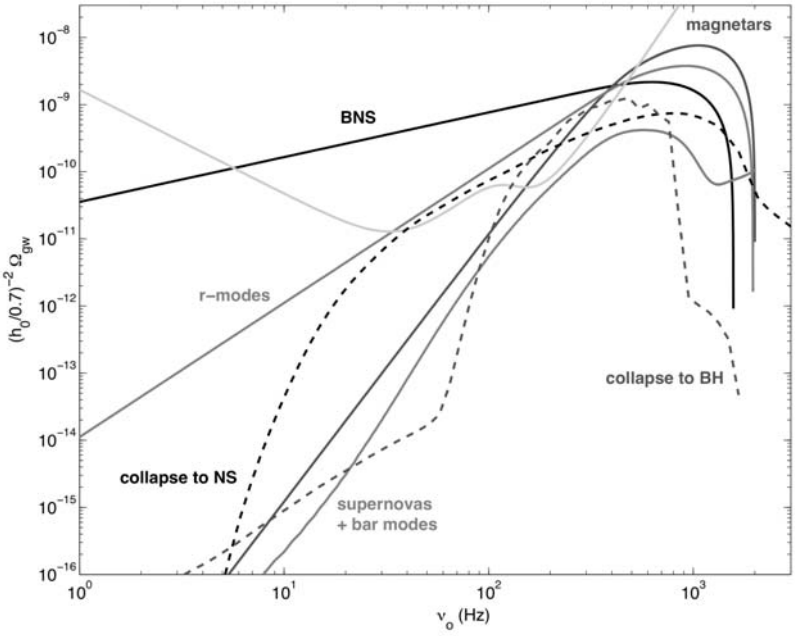

Fig. 6 Energy density of the most promising astrophysical background contributions for ground based detectors, discussed in the text: magnetars (threshold detectable by ET), binary neutron stars, dynamical bar modes in proto-neutron stars (courtesy of E. Howell), r-modes assuming that 1% of newborn neutron stars cross the instability window, Population II core collapse to neutron stars (model of Ott et al. 2006) and to black holes (model D5a of Sekiguchi & Shibata 2005), courtesy of S. Marrasi.

1995; Ando 2004; de Freitas Pacheco et al. 2006; Belczynski et al. 2006; O'Shaughnessy et al. 2008) suggest that the delay time is well described by a probability distribution of the form

$$P_{\rm d}(t_{\rm d}) \propto \frac{1}{t_{\rm d}} \text{ with } t_{\rm d} > \tau_0. \tag{19}$$

This broad model accounts for the wide range of merger times observed in binary pulsars and is also consistent with short gamma ray burst observations in both late and early type galaxies (Berger et al. 2007). Belczyński & Kalogera (2001) and Belczynski et al. (2006) have identified a new efficient formation channel which produces a significant fraction of tight binaries with merger times in the range $\tau_m \sim 0.001-0.1\,$Myr, which gives a minimal delay time $\tau_0 \sim 20\,$Myr, corresponding roughly to the time it takes for massive binaries to evolve into two neutron stars.

The local cosmological rate at $z = 0$, $\dot{\rho}_{\rm o}$ in $\rm Myr^{-1}\,Mpc^{-3}$, is usually extrapolated by taking the product of the rate in the Milky Way ($r_{\rm mw}$ in $\rm yr^{-1}$) and the density of Milky Way equivalent galaxies, given from measurements of the blue stellar luminosity around $n_{\rm mw} \sim (1-2)\times 10^{-2}\,\rm Mpc^{-3}$ (Phinney 1991; Kalogera et al. 2001; Kopparapu et al. 2008). The most current estimates of the NS-NS galactic coalescence rate are given in the range $1-817\,\rm Myr^{-1}$ (95% confidence intervals) for statistical studies which extrapolate the rates from observed galactic NS–NS occurrences (Kalogera et al. 2004), preferably between $17-292$ (95% confidence interval) with a peak probability around $83\,\rm Myr^{-1}$, and in the range $1-300$, but more likely around $10-30$, for population synthesis models which combine theoretical and observational constraints (Table 4). In the quadrupolar approximation, the GW energy spectrum emitted by a binary system, which inspirals in a circular orbit, is given

Table 4 Taken from table 4 of Postnov & Yungelson (2006), the most current estimates of the Galactic merger rates of NS-NSs and NS-BHs, derived from statistical studies (first row), and from population synthesis. The high rate obtained by Tutunov and Yungelson (1993) is due to the assumption that neutron stars or black holes are born with no kick velocity, leading to an overestimate of the number of systems that survive the two supernovae. The low rate obtained by Voss and Tauris (2003) is due to the use of a different value of the parameter λ, which measures the binding energy of the common envelop.

Statistics	NS-NS	
Kalogera et al. (2004)	83 (17–292)	
Population Synthesis	NS–NS	NS–BH
Tutunov and Yungelson (1993)	300	20
Lipunov et al. (1997)	30	2
Potergies Zwart and Yungelson (1998)	20	2
Nelemans et al. (2001)	20	4
Voss and Tauris (2003)	2	0.6
O'Shaughnessy et al. (2005)	7	1
de Freitas Pacheco et al. (2006)	17	
Belczinsky et al. (2007)	10–15	0.1
O'Shaughnessy et al. (2008)	30	3

up to the last stable orbit $\nu_{\max}$ by

$$dE_{\rm gw}/d\nu = \frac{(G\pi)^{2/3}}{3}\frac{m_1 m_2}{(m_1+m_2)^{1/3}}\nu^{-1/3}. \tag{20}$$

Assuming $m_1 = m_2 = 1.4\,M_\odot$ for the star masses, and replacing the equations above in Equation (8), we find that the energy density increases as $\Omega_{\rm gw} \sim \dot{\rho}_0 \nu_{\rm o}^{2/3}$ before it reaches a maximum of $\sim 2\times10^{-9}\dot{\rho}_0$ around 600 Hz. This means that the Einstein Telescope should be able to detect the background from binaries even for the most pessimistic predictions of the coalescence rate, down to $\dot{\rho}_0 \sim 0.035$ (roughly equivalent to a galactic rate of $3\,{\rm Myr}^{-1}$), for a signal-to-noise ratio of 3 and one year of observation (T=1 yr).

5.2 Rotating Neutron Stars: Tri-axial Emission

Rotating neutron stars with a triaxial shape may have a time varying quadrupole moment and hence radiate GWs at twice the rotational frequency. The total spectral gravitational energy emitted by a neutron star born with a rotational period P_0, and which decelerates through magnetic dipole torques and GW emission, is given by

$$\frac{dE_{\rm gw}}{d\nu} = K\nu^3\Big(1+\frac{K}{\pi^2 I_{zz}}\nu^2\Big)^{-1} \text{ with } \nu\in[0-2/P_0], \tag{21}$$

where

$$K = \frac{192\pi^4 G I^3}{5c^5R^6}\frac{\varepsilon^2}{B^2}. \tag{22}$$

R is the radius of the star, $\varepsilon = (I_{xx}-I_{yy})/I_{zz}$ is the ellipticity, I_{ij} is the principal moment of inertia, and B is the projection of the magnetic dipole in the direction orthogonal to the rotation axis. Since the evolution of massive stars that give birth to pulsars is very fast, the rate can be derived directly from the star formation rate (see Eq. (11)). Considering the interval $8-40\,M_\odot$ for the mass range of neutron star progenitors, and the initial mass function of Equation (12), Regimbau & Mandic (2008) found $\lambda \sim 9\times10^{-3}\,M_\odot^{-1}$.

Normal radio pulsars, which are born with magnetic fields on the order of $10^{12}-10^{13}$ G, and rotational periods on the order of tens or hundreds of milliseconds (Regimbau & de Freitas Pacheco

2000; Faucher-Giguère & Kaspi 2006; Soria et al. 2008), are not expected to contribute significantly to the GW signal (Regimbau & de Freitas Pacheco 2001b). However, the population of newborn magnetars in which super-strong crustal magnetic fields ($B \sim 10^{14} - 10^{16}$ G) may have been formed by dynamo action in a proto-neutron star with a very small rotational period (on the order of 1 ms) (Duncan & Thompson 1992; Thompson & Duncan 1993), may produce a strong stochastic background in the frequency band of terrestrial detectors (Regimbau & de Freitas Pacheco 2006a). For these highly magnetized neutron stars, the distortion induced by the magnetic torque becomes significant, strongly enhancing the GW emission. In the case of a pure poloidal internal magnetic field matching the dipolar field B in the exterior region, the ellipticity is given by Bonazzola & Gourgoulhon (1996) and Konno et al. (2000)

$$\varepsilon_B = \beta \frac{R^8 B^2}{4GI_{zz}^2}, \tag{23}$$

where β is a distortion parameter which depends on both the equation of state and the magnetic field geometry. Using numerical simulations, Bonazzola & Gourgoulhon (1996) found that β can range between $1 - 10$ for a non-superconducting interior to $100 - 1000$ for a type I superconductor and even take values larger than $1000 - 10\,000$ for a type II superconductor with counter rotating electric currents. Taking $R = 10$ km for the radius, $I_{zz} = 1.4 \times 10^{45}$ g cm^2 for the moment of inertia, and assuming that magnetars represent 10% of the population of NSs (Kouveliotou et al. 1998), we find that the stochastic signal is detectable with the Einstein Telescope after an observation time $T = 1$ yr and with a signal to noise ratio of 3 when $\frac{\varepsilon}{B} > 1.5 \times 10^{-18}$ or $\beta B > 8 \times 10^{17}$, giving researchers the opportunity to put very interesting constraints on both B and β. On the other hand, it has been suggested that the spindown could become purely gravitational if the internal magnetic field could be dominated by a very strong toroidal component (Cutler 2002; Stella et al. 2005), on the order of 10^{16} G. In this saturation regime, the energy density increases as $\nu_{\rm o}^2$ at low frequencies and reaches a maximum of $\Omega_{\rm gw} \sim 1.3 \times 10^{-8}$ around 1600 Hz, giving a signal detectable by the Einstein Telescope with a signal-to-noise ratio of 45.

5.3 Rotating Neutron Stars: Initial Instabilities

5.3.1 Dynamical bar modes

The gravitational stochastic background from core collapse supernovae could be enhanced by a number of proposed post-collapse emission mechanisms. One intriguing mechanism is the bar-mode dynamical instability associated with neutron star formation. These instabilities derive their name from the 'bar-like' deformation they induce, transforming a disk-like body into an elongated bar that tumbles end-over-end. The highly non-axisymmetric structure resulting from a compact astrophysical object encountering this instability makes such an object a potentially strong source of gravitational radiation and has been the subject of a number of numerical studies (Brown 2000; New et al. 2000; Shibata et al. 2000; Saijo et al. 2001; Baiotti et al. 2007). Howell (2010) have calculated the resulting background signal from this emission process using simulated energy spectra data, $dE_{\rm gw}/d\nu$, from Shibata & Sekiguchi (2005), who performed the first three dimensional hydrodynamic simulations for stellar core collapses in full general relativity. Assuming a 20% occurrence of this instability, the authors found that the density parameter reaches a maximum of $\Omega_{\rm gw} \sim 4 \times 10^{-10}$ around 600 Hz, and may be detectable with the Einstein Telescope with a signal to noise ratio of 3 after one year of integration. The optimistic event rate considered by Howell et al. is supported by suggestions that post-collapse neutrino emission by the proto-neutron stars can induce contraction through cooling. This leads to increased spins though conservation of angular momentum (Shibata & Sekiguchi 2005). The implication here is that the instability can set in tens of milliseconds post-collapse, increasing the rate of occurrence.

5.3.2 r-modes

The stochastic background from r-modes was first investigated by Owen et al. (1998) and then reviewed by Ferrari et al. (1999b). These estimates are based on the initial model of Lindblom et al. (1998), which does not account for dissipation mechanisms such as the effect of the solid crust or the magnetic field, which may significantly reduce the gravitational instability. The spectral energy density of a single source is given by

$$\frac{dE_{\rm gw}}{d\nu} = \frac{2E_o}{\nu_{\rm sup}^2}\nu \text{ with } \nu \in [0 - \nu_{\rm sup}], \tag{24}$$

where $\nu_{\rm sup}$ is 4/3 of the initial rotational frequency and E_0 is the rotational energy lost within the instability window. For NSs with radius $R = 10$ km and mass $M = 1.4\,M_\odot$, the spectrum evolves as $\Omega_{\rm gw} \sim 10^{-12}\xi\nu_{\rm o}^3$ where ξ is the fraction of NSs born near the Keplerian velocity and which enters the instability window, until it reaches a maximum at 900 Hz. The Einstein Telescope may be able to detect this signal with a signal to noise ratio larger than > 3 for $T = 1$ yr if $\xi > 0.23\%$. One obtains similar constraints with the secular bar mode instability at the transition between Maclaureen and Dedekind configurations (Lai & Shapiro 1995).

5.3.3 Collapse to quark matter

It has been suggested that neutron stars could also undergo small core collapses after phase transitions, producing large amounts of gravitational waves. Sigl (2006) calculated the background from phase transition to quark matter in newly born NSs with millisecond periods, based on recent numerical simulations (Lin et al. 2006). Assuming that 1% of neutron stars are born fast enough to undergo the phase transition, and that the energy released in the process represents about 5% of the rotational energy ($\sim 2 \times 10^{51}$ erg), the energy density parameter may reach a maximum of $\Omega_{\rm gw} \sim 10^{-10}$ at kHz frequencies.

5.4 Core Collapse Supernovae

5.4.1 Core collapse supernovae to neutron stars

After they have burnt all their combustible nuclear fuel, massive stars may explode as type II supernovae. Their envelope is ejected while the core collapses to form an NS or a BH, depending on the initial mass of the progenitor, emitting a large amount of gravitational waves in the process. In a recent work, Howell et al. (2004) calculated the stochastic background that results from the birth of neutron stars at cosmological distances, using relativistic numerical models of core collapse (Dimmelmeier et al. 2002), and updating the previous study by Coward et al. (2001), based on Newtonian models (Zwerger & Mueller 1997). They considered three different GW waveforms, assumed to be representative of the three types of catalogs. Type I waveforms are characterized by a spike resulting from the core bounce followed by a ringdown, Type II by several distinct spikes and Type III shows large positive and smaller negative amplitudes just before and after bounce. In order to calculate the background spectrum, they assumed a flat cosmology, with $\Omega_m = 0.3$, $\Omega_\Lambda = 0.7$ and Hubble parameter $H_0 = 70\,{\rm km\,s^{-1}\,Mpc^{-1}}$ (the 737 cosmology Rao et al. 2006), corresponding to the so-called concordant model derived from observations of distant type Ia supernovae (Perlmutter et al. 1999) and the power spectra of the cosmic microwave background fluctuations (Spergel et al. 2003), and considered three different models of the SFRs, finding no significant difference in the results. The NS progenitors were assumed to have masses between $8 - 25\,M_\odot$ for a Salpeter IMF normalized between $0.1 - 125\,M_\odot$. The background is found to be continuous for Type II and is rather like popcorn noise for Type I and III waveforms. The energy density parameter reaches a

maximum of $\Omega_{\rm gw} \sim 3 \times 10^{-12}$ around 700 Hz for Type I and $\Omega_{\rm gw} \sim 10^{-13}$ at 100 Hz and 800 Hz for Type II and Type III respectively.

Besides the emission from the supernova bounce signal in the kHz range, it is expected that the large-scale convective overturn, that develops in the delayed explosion scenario during the epoch of shock-wave stagnation, may emit a much stronger signal that may last for a few hundreds of ms before the actual explosion in the 1 Hz frequency range. Buonanno et al. (2005) estimated the background produced by both ordinary supernovae and Pop III stars using different numerical models of the GW waveform (Fryer et al. 2004; Müller et al. 2004). They showed that the signal is Gaussian below 1 Hz with an amplitude that may be at the level of the background expected from inflationary models. However, the authors stressed that these estimates remain uncertain by several orders of magnitude, essentially due to uncertainties in the parameters of the supernova GW emission.

5.4.2 Core collapse supernovae to black holes

The GW background from core collapse supernovae that result in the formations of black holes was first investigated by Ferrari et al. (1999a), using the relativistic numerical simulations of Stark & Piran (1985, 1986) and later by de Araujo et al. (2002a) who found similar results assuming that all the energy goes into the ringdown of the $l = m = 2$ dominant quasi-normal mode. For this mode, the frequency is given by (Echeverria 1989)

$$\nu_*(m, a) \approx \frac{\Delta(a)}{\alpha m(M_\odot)}, \tag{25}$$

with

$$\Delta(a) = \frac{c^3}{2\pi G}\left[1 - 0.63(1-a)^{0.3}\right], \tag{26}$$

where M is the mass of the black hole, assumed to be a fraction α of the mass of the progenitor m, and a the dimensionless spin factor, ranging from 0 for a Schwarzschild BH to 1 in the extreme Kerr limit. The spectral energy density has the simple expression:

$$\frac{dE_{\rm gw}}{d\nu} = \varepsilon \alpha m c^2 \delta(\nu - \nu_*(M)), \tag{27}$$

where ε is an efficiency coefficient. Numerical simulations of Stark & Piran (1985) give an upper limit of $\varepsilon \sim 7 \times 10^{-4}$ for an axisymmetric collapse, but accounting for more realistic scenarios, in particular the pressure reduction that triggers the collapse, Baiotti & Rezzolla (2006) obtained an efficiency on the order of $10^{-7} - 10^{-6}$, 2–3 orders of magnitude smaller. Assuming that stars in the range $30 - 100\,M_\odot$ can produce a BH, taking $\alpha = 10\%$ and $a = 0.6$, this simple model gives the energy density ranges between $0.25 - 5.6$ kHz, with a maximum of $\Omega_{\rm gw} \sim \varepsilon \times 10^{-8}$ around 1650 Hz, which means that an efficiency $> 2 \times 10^{-3}$ would produce a detectable signal with a signal to noise ratio of 3 after one year of observation with the Einstein Telescope. Decreasing the minimal mass or α would narrow the spectrum and shift the maximum toward lower frequencies, while a change in the efficiency parameter ε would only affect the amplitude. Increasing the spin factor or broadening its distribution broadens the spectrum and shifts the maximum toward larger frequencies. Taking $\alpha = 20\%$, we find that the signal is detectable for efficiencies larger than 0.01%.

In a recent work, Marassi et al. (2009) made use of the recent progress in numerical relativity, to review and extend the previous estimates of Ferrari et al. (1999a) for both Population II and Population III stars. The supernova rates were derived from the numerical simulations of Tornatore et al. (2007), which follow the star's evolution, metal enrichment and energy deposition, and the GW signal's waveform was derived from relativistic numerical simulations. The background is out of reach of the first generation of detectors for Pop III stellar collapses, but could be detected by the Einstein Telescope for Pop II supernovae. Assuming $20 - 100\,M_\odot$ for the mass range of BH

progenitors, they found that the energy density reaches a maximum of $\Omega_{\rm gw} \sim 4 - 7 \times 10^{-10}$ around 500 Hz for the model of Sekiguchi & Shibata (2005), giving a signal to noise ratio between $1.6-7.1$ after one year of observation. In addition, they estimated the background from the collapsed neutron stars. Assuming $8 - 20\,M_\odot$ for the mass of the progenitors, and the model of Ott (2005) which accounts for the g-mode excitation, they found that the energy density reaches a maximum $\Omega_{\rm gw} \sim 10^{-9}$ around 1000 Hz, giving a signal to noise ratio of 8.2.

Similarly, Zhu, Howell & Blair (2010) estimated the GW signal created by all core collapse supernovae, to NSs and BHs, using a Gaussian spectrum of the form

$$\frac{dE_{\rm gw}}{d\nu} = A \exp(-(\nu - \nu_*)/2\sigma^2) \tag{28}$$

shown to be a good approximation of the models of Ott et al. (2006). Based on simulated spectra of Dimmelmeier et al. (2008) and Sekiguchi & Shibata (2005), they considered $\sim$500 and $\nu_* = 200 - 800$ Hz. They found that the signal may be detectable for efficiencies $\varepsilon > 10^{-5}$ and $\varepsilon > 10^{-7}$ for the Einstein Telescope.

5.5 Capture by Supermassive Black Holes

The emission from the various populations of compact binaries, which represents the main source of confusion noise for LISA, was studied intensively in the past decades (see for instance Kosenko & Postnov 1998; Ignatiev et al. 2001; Schneider et al. 2001; Farmer & Phinney 2002; Cooray 2004 for the extra-galactic contribution). The signal is expected to be largely dominated by white dwarf-white dwarf (WD-WD) interactions, and in particular by the galactic population between $0.1 - 10$ (Yungelson et al. 2001; Nelemans et al. 2001; Benacquista et al. 2004; Edlund et al. 2005; Belczynski et al. 2005; Timpano et al. 2006; Benacquista & Holley-Bockelmann 2006). In a recent paper, Barack & Cutler (2004) investigated the stochastic background created by unresolved captures by supermassive black holes (SMBHs) (Amaro-Seoane et al. 2007). The capture rates for WDs, NSs and stellar BHs, which were extrapolated from the rates derived by Freitag (2003) for our galaxy, represent the main source of uncertainties, ranging between $4 \times 10^{-8} - 4 \times 10^{-6}\,M_6^{3/8}$ yr^{-1} for WD captures and between $6 \times 10^{-8} - 6 \times 10^{-7}\,M_6^{3/8}$ yr^{-1} for NS and BH captures, with M_6 being the mass of the SMBH in units of $10^6\,M_\odot$. In Figure 7, the most optimistic and pessimistic models are compared to the LISA instrumental noise and to the WD-WD galactic foreground derived by Bender & Hils (1997). For the most optimistic rates, the resulting background may contribute to the LISA confusion noise, raising LISA's effective overall noise level by a factor of ~ 2 in the range $1 - 10$ mHz, where LISA is most sensitive.

6 CONCLUSIONS AND FUTURE PROSPECTS

Ground based GW experiments, after a decade of detector installation and commissioning, have reached or surpassed their design sensitivities, opening a new window into the Universe. The first generation LIGO interferometers has already put interesting astrophysical constraints on the ellipticity of the Crab pulsar (below the spindown limit). With advanced detectors, we expect to see at least close compact binary coalescences, while the third generation detector of the Einstein Telescope and the space detector LISA should bring GW astronomy to the next level, when it will not only be possible to address a range of problems from a wide variety of astrophysical sources, but also those from fundamental physics and cosmology.

The cosmological stochastic background is often seen as the Holy Grail of GW astronomy since it would give a snapshot of the very early stages of the Universe, up to a fraction of a second after the Big Bang. The astrophysical background is also promising since it would provide information on the physical properties of compact objects and their evolution with redshift, such as the mass of neutron

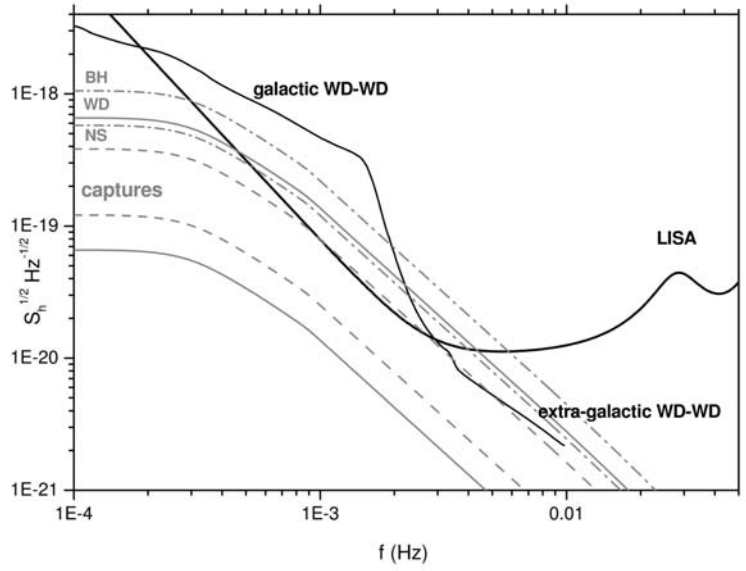

Fig. 7 Gravitational strain in $\mathrm{Hz}^{-1/2}$, corresponding to optimistic (*grey curve*) and pessimistic (*grey dashed curve*) compact object captures (Barack & Cutler 2004), along with the LISA instrumental noise (*black*) and the WD-WD foreground (*black*).

stars or black holes, the ellipticity and the magnetic field of neutron stars, the angular momentum of black holes, and the rate of occurrence of compact binaries. We have shown in the previous sections that astrophysical models are out of reach of the first generation of detectors but with advanced detectors, particularly the third generation Einstein Telescope, the derived upper limits could put very interesting constraints on the equation of state and magnetic field of magnetars, the distribution of the birth rotation period of newborn neutron stars and models of core collapse supernovae. Moreover, unless we overestimate the rate by orders of magnitude, we should be able to see the background from coalescing double neutron star binaries.

On the other hand, the astrophysical contribution may be a noise masking the cosmological background, and also a confusion foreground where the detection of individual high-redshift standard candles needed to infer dark energy may become difficult to decern (Regimbau & Hughes 2009). In this context, modeling the astrophysical background as precisely as possible to extract information on its strength, frequency range and statistical properties, anything that may help distinguish it from the cosmological signal or separate overlapping sources, is crucial.

Another important task in the next few years will be to adapt our actual methods to the triangle configurations of the ET and the spatial interferometer LISA. It is not yet certain that we can ever get rid of the correlated noise, but we should certainly be able to reduce it by correlating interferometers formed by specific combinations of the three arms, with the extra complication for LISA that the triangle is moving.

Acknowledgements The author thanks Vuk Mandic for providing the landscape plot for the cosmological background, and Eric Howell and Stefania Marassi for their contribution to the bar mode instability and the core collapse supernovae sections.

References

Abbott, B., Abbott, R., Adhikari, R., et al. 2004, Phys. Rev. D, 69, 122004
Abbott, B., Abbott, R., Adhikari, R., et al. 2005, Physical Review Letters, 95, 221101
Abbott, B., Abbott, R., Adhikari, R., et al. 2007, ApJ, 659, 918
Abbott, B. P., Abbott, R., Acernese, F., et al. 2009, Nature, 460, 990
Abramovici, A., Althouse, W. E., Drever, R. W. P., et al. 1992, Science, 256, 325
Allen, B. 1997, in Relativistic Gravitation and Gravitational Radiation, eds. J.-A. Marck, & J.-P. Lasota, 373
Allen, B., & Ottewill, A. C. 1997, Phys. Rev. D, 56, 545
Allen, B., & Romano, J. D. 1999, Phys. Rev. D, 59, 102001
Amaldi, E., Astone, P., Bassan, M., et al. 1990, Europhysics Letters, 12, 5
Amaro-Seoane, P. et al. 2007, Classical and Quantum Gravity, 24, 17
Ando, S. 2004, J. Cosmol. Astropart. Phys., 6, 7
Arnaud, N., Cavalier, F., Davier, M., & Hello, P. 1999, Phys. Rev. D, 59, 082002
Astone, P., Bassan, M., Bonifazi, P., et al. 1999, A&A, 351, 811
Avelino, P. P., Shellard, E. P. S., Wu, J. H. P., & Allen, B. 1998, Physical Review Letters, 81, 2008
Baiotti, L., & Rezzolla, L. 2006, Physical Review Letters, 97, 141101
Baiotti, L., de Pietri, R., Manca, G. M., & Rezzolla, L. 2007, Phys. Rev. D, 75, 044023
Ballmer, S. W. 2006, Classical and Quantum Gravity, 23, 179
Barack, L., & Cutler, C. 2004, Phys. Rev. D, 70, 122002
Battye, R. A., Caldwell, R. R., & Shellard, E. P. S. 1998, in Topological Defects in Cosmology, eds. M. Signore, & F. Melchiorri, 11
Belczynski, K., Benacquista, M., Larson, S. L., & Ruiter, A. J. 2005, arXiv:astro-ph/0510718
Belczyński, K., & Kalogera, V. 2001, ApJ, 550, L183
Belczynski, K., Perna, R., Bulik, T., et al. 2006, ApJ, 648, 1110
Benacquista, M., & Holley-Bockelmann, K. 2006, ApJ, 645, 589
Benacquista, M. J., DeGoes, J., & Lunder, D. 2004, Classical and Quantum Gravity, 21, 509
Bender, P. L., & Hils, D. 1997, Classical and Quantum Gravity, 14, 1439
Bender, P. L., & the LISA Study Team 1998, Laser Interferometer Space Antenna for the Detection of Gravitational Waves, Pre-Phase A Report, MPQ233 (Max-Plank-Institüt für Quantenoptik, Garching)
Berger, E., Fox, D. B., Price, P. A., et al. 2007, ApJ, 664, 1000
Blain, A. W., Kneib, J., Ivison, R. J., & Smail, I. 1999, ApJ, 512, L87
Blair, D., & Ju, L. 1996, MNRAS, 283, 648
Blair, D. G., Ivanov, E. N., Tobar, M. E., et al. 1995, Physical Review Letters, 74, 1908
Bonazzola, S., & Gourgoulhon, E. 1996, A&A, 312, 675
Bradaschia, C., del Fabbro, R., di Virgilio, A., et al. 1990, Nuclear Instruments and Methods in Physics Research A, 289, 518
Brown, J. D. 2000, Phys. Rev. D, 62, 084024
Buonanno, A. 2003, arXiv:gr-qc/0303085
Buonanno, A., Maggiore, M., & Ungarelli, C. 1997, Phys. Rev. D, 55, 3330
Buonanno, A., Sigl, G., Raffelt, G. G., Janka, H., & Müller, E. 2005, Phys. Rev. D, 72, 084001
Caprini, C. 2010, arXiv:1005.5291
Cerdonio, M., Bonaldi, M., Carlesso, D., et al. 1997, Classical and Quantum Gravity, 14, 1491
Cole, S., Norberg, P., Baugh, C. M., et al. 2001, MNRAS, 326, 255
Cooray, A. 2004, MNRAS, 354, 25
Cornish, N. J. 2001, Classical and Quantum Gravity, 18, 4277
Coward, D., & Regimbau, T. 2006, New Astron. Rev., 50, 461
Coward, D. M., & Burman, R. R. 2005, MNRAS, 361, 362

Coward, D. M., Burman, R. R., & Blair, D. G. 2001, MNRAS, 324, 1015
Coward, D. M., Burman, R. R., & Blair, D. G. 2002, MNRAS, 329, 411
Cutler, C. 2002, Phys. Rev. D, 66, 084025
Cyburt, R. H., Fields, B. D., Olive, K. A., & Skillman, E. 2005, Astroparticle Physics, 23, 313
Damour, T., & Vilenkin, A. 2000, Physical Review Letters, 85, 3761
Damour, T., & Vilenkin, A. 2001, Phys. Rev. D, 64, 064008
Damour, T., & Vilenkin, A. 2005, Phys. Rev. D, 71, 063510
de Araujo, J. C. N., Miranda, O. D., & Aguiar, O. D. 2000, Nuclear Physics B Proceedings Supplements, 80, C702
de Araujo, J. C. N., Miranda, O. D., & Aguiar, O. D. 2002a, Classical and Quantum Gravity, 19, 1335
de Araujo, J. C. N., Miranda, O. D., & Aguiar, O. D. 2002b, MNRAS, 330, 651
de Araujo, J. C. N., Miranda, O. D., & Aguiar, O. D. 2004, MNRAS, 348, 1373
de Freitas Pacheco, J. A., Regimbau, T., Vincent, S., & Spallicci, A. 2006, International Journal of Modern Physics D, 15, 235
Dimmelmeier, H., Font, J. A., & Müller, E. 2002, A&A, 393, 523
Dimmelmeier, H., Ott, C. D., Marek, A., & Janka, H.-T. 2008, Phys. Rev. D, 78, 064056
Drasco, S., & Flanagan, É. É. 2003, Phys. Rev. D, 67, 082003
Duncan, R. C., & Thompson, C. 1992, ApJ, 392, L9
Echeverria, F. 1989, Phys. Rev. D, 40, 3194
Edlund, J. A., Tinto, M., Królak, A., & Nelemans, G. 2005, Phys. Rev. D, 71, 122003
Fardal, M. A., Katz, N., Weinberg, D. H., & Davé, R. 2007, MNRAS, 379, 985
Farmer, A. J., & Phinney, E. S. 2002, in Bulletin of the American Astronomical Society 34, 1225
Faucher-Giguère, C., & Kaspi, V. M. 2006, ApJ, 643, 332
Ferrari, V., Matarrese, S., & Schneider, R. 1999a, MNRAS, 303, 247
Ferrari, V., Matarrese, S., & Schneider, R. 1999b, MNRAS, 303, 258
Flanagan, E. E. 1993, Phys. Rev. D, 48, 2389
Freitag, M. 2003, ApJ, 583, L21
Fryer, C. L., Holz, D. E., & Hughes, S. A. 2004, ApJ, 609, 288
Gasperini, M., & Veneziano, G. 1993, Astroparticle Physics, 1, 317
Gasperini, M., & Veneziano, G. 2003, Phys. Rep., 373, 1
Grishchuk, L. P. 1974, Soviet Journal of Experimental and Theoretical Physics, 40, 409
Grishchuk, L. P. 1993, Classical and Quantum Gravity, 10, 2449
Grishchuk, L. P., Lipunov, V. M., Postnov, K. A., Prokhorov, M. E., & Sathyaprakash, B. S. 2001, Physics Uspekhi, 44, 1
Hopkins, A. M., & Beacom, J. F. 2006, ApJ, 651, 142
Hough, J. 1992, in Marcel Grossmann Meeting on General Relativity, 192
Hough, J., Pugh, J. R., Bland, R., & Drever, R. W. P. 1975, Nature, 254, 498
Howell, E. 2010, PhD Thesis, School of Physics, The University of Western Australia
Howell, E., Coward, D., Burman, R., Blair, D., & Gilmore, J. 2004, MNRAS, 351, 1237
Ignatiev, V. B., Kuranov, A. G., Postnov, K. A., & Prokhorov, M. E. 2001, MNRAS, 327, 531
Jenet, F. A., Hobbs, G. B., Lee, K. J., & Manchester, R. N. 2005, ApJ, 625, L123
Kalogera, V., Kim, C., Lorimer, D. R., et al. 2004, ApJ, 614, L137
Kalogera, V., Narayan, R., Spergel, D. N., & Taylor, J. H. 2001, ApJ, 556, 340
Kaspi, V. M., Taylor, J. H., & Ryba, M. F. 1994, ApJ, 428, 713
Konno, K., Obata, T., & Kojima, Y. 2000, A&A, 356, 234
Kopparapu, R. K., Hanna, C., Kalogera, V., et al. 2008, ApJ, 675, 1459
Kosenko, D. I., & Postnov, K. A. 1998, A&A, 336, 736
Kouveliotou, C., Dieters, S., Strohmayer, T., et al. 1998, Nature, 393, 235

Kuroda, K., Kanda, N., Ohashi, M., et al. 2006, Progress of Theoretical Physics Supplement, 163, 54
Lai, D., & Shapiro, S. L. 1995, ApJ, 442, 259
Lin, L., Cheng, K. S., Chu, M., & Suen, W. 2006, ApJ, 639, 382
Lindblom, L., Owen, B. J., & Morsink, S. M. 1998, Physical Review Letters, 80, 4843
Lipunov, V. M., Postnov, K. A., Prokhorov, M. E., Panchenko, I. E., & Jorgensen, H. E. 1995, ApJ, 454, 593
Lommen, A. N., Backer, D. C., Splaver, E. M., & Nice, D. J. 2003, in Astronomical Society of the Pacific Conf. Ser. 302, Radio Pulsars, eds. M. Bailes, D. J. Nice, & S. E. Thorsett, 81
Madau, P., Pozzetti, L., & Dickinson, M. 1998, ApJ, 498, 106
Maggiore, M. 2000, Phys. Rep., 331, 283
Manchester, R. N. 2006, ChJAA (Chin. J. Astron. Astrophys.), 6S, 139
Mandic, V., & Buonanno, A. 2006, Phys. Rev. D, 73, 063008
Marassi, S., Schneider, R., & Ferrari, V. 2009, MNRAS, 398, 293
Mauceli, E., Geng, Z. K., Hamilton, W. O., et al. 1996, Phys. Rev. D, 54, 1264
Mitra, S., Dhurandhar, S., Souradeep, T., et al. 2008, Phys. Rev. D, 77, 042002
Müller, E., Rampp, M., Buras, R., Janka, H., & Shoemaker, D. H. 2004, ApJ, 603, 221
Nagamine, K., Ostriker, J. P., Fukugita, M., & Cen, R. 2006, ApJ, 653, 881
Nelemans, G., Yungelson, L. R., Portegies Zwart, S. F., & Verbunt, F. 2001, A&A, 365, 491
New, K. C. B., Centrella, J. M., & Tohline, J. E. 2000, Phys. Rev. D, 62, 064019
O'Shaughnessy, R., Belczynski, K., & Kalogera, V. 2008, ApJ, 675, 566
Ott, C. D., Burrows, A., Dessart, L., & Livne, E. 2006, Physical Review Letters, 96, 201102
Ott, C. D., Ou, S., Tohline, J. E., & Burrows, A. 2005, ApJ, 625, L119
Owen, B. J., Lindblom, L., Cutler, C., et al. 1998, Phys. Rev. D, 58, 084020
Pallottino, G. V. 1997, in Gravitational Waves: Sources and Detectors, eds. I. Ciufolini & F. Fidecaro, 159
Perlmutter, S., Aldering, G., Goldhaber, G., et al. 1999, ApJ, 517, 565
Phinney, E. S. 1991, ApJ, 380, L17
Piran, T. 1992, ApJ, 389, L45 or Rebolo, R., Martin, E. L., & Magazzu, A. 1992, ApJ, 389, L83
Postnov, K. A., & Yungelson, L. R. 2006, Living Reviews in Relativity, 9, 6
Pradier, T., Arnaud, N., Bizouard, M., et al. 2001, Phys. Rev. D, 63, 042002
Rao, S. M., Turnshek, D. A., & Nestor, D. B. 2006, ApJ, 636, 610
Regimbau, T. 2007, Phys. Rev. D, 75, 043002
Regimbau, T., & de Freitas Pacheco, J. A. 2000, A&A, 359, 242
Regimbau, T., & de Freitas Pacheco, J. A. 2001a, A&A, 374, 182
Regimbau, T., & de Freitas Pacheco, J. A. 2001b, A&A, 376, 381
Regimbau, T., & de Freitas Pacheco, J. A. 2006a, A&A, 447, 1
Regimbau, T., & de Freitas Pacheco, J. A. 2006b, ApJ, 642, 455
Regimbau, T., & Hughes, S. A. 2009, Phys. Rev. D, 79, 062002
Regimbau, T., & Mandic, V. 2008, Classical and Quantum Gravity, 25, 184018
Saijo, M., Shibata, M., Baumgarte, T. W., & Shapiro, S. L. 2001, ApJ, 548, 919
Salpeter, E. E. 1955, ApJ, 121, 161
Schneider, R., Ferrari, V., Matarrese, S., & Portegies Zwart, S. F. 2001, MNRAS, 324, 797
Schnittman, J., Sigl, G., & Buonanno, A. 2006, in American Institute of Physics Conf. Ser. 873, Laser Interferometer Space Antenna, eds. S. M. Merkovitz & J. C. Livas, 437
Sekiguchi, Y., & Shibata, M. 2005, Phys. Rev. D, 71, 084013
Shibata, M., Baumgarte, T. W., & Shapiro, S. L. 2000, ApJ, 542, 453
Shibata, M., & Sekiguchi, Y. 2005, Phys. Rev. D, 71, 024014
Siemens, X., Mandic, V., & Creighton, J. 2007, Physical Review Letters, 98, 111101
Sigl, G. 2006, J. Cosmol. Astropart. Phys., 4, 2
Smith, T. L., Pierpaoli, E., & Kamionkowski, M. 2006, Physical Review Letters, 97, 021301

Soria, R., Perna, R., Pooley, D., & Stella, L. 2008, arXiv:0811.3605
Spergel, D. N., Verde, L., Peiris, H. V., et al. 2003, ApJS, 148, 175
Stark, R. F., & Piran, T. 1985, Physical Review Letters, 55, 891
Stark, R. F., & Piran, T. 1986, in Fourth Marcel Grossmann Meeting on General Relativity, ed. R. Ruffini, 327
Starobinskiĭ, A. A. 1979, Soviet Journal of Experimental and Theoretical Physics Letters, 30, 682
Steidel, C. C., Adelberger, K. L., Giavalisco, M., Dickinson, M., & Pettini, M. 1999, ApJ, 519, 1
Stella, L., Dall'Osso, S., Israel, G. L., & Vecchio, A. 2005, ApJ, 634, L165
Thompson, C., & Duncan, R. C. 1993, ApJ, 408, 194
Timpano, S. E., Rubbo, L. J., & Cornish, N. J. 2006, Phys. Rev. D, 73, 122001
Tong, M. L., & Zhang, Y. 2009, Phys. Rev. D, 80, 084022
Tornatore, L., Borgani, S., Dolag, K., & Matteucci, F. 2007, MNRAS, 382, 1050
Tutukov, A. V., & Yungelson, L. R. 1993, MNRAS, 260, 675
Tutukov, A. V., & Yungelson, L. R. 1994, MNRAS, 268, 871
Vilenkin, A., & Shellard, E. P. S. 2000, Cosmic Strings and Other Topological Defects
Voss, R., & Tauris, T. M. 2003, MNRAS, 342, 1169
Wilkins, S. M., Trentham, N., & Hopkins, A. M. 2008, MNRAS, 385, 687
Yungelson, L. R., Nelemans, G., Portegies Zwart, S. F., & Verbunt, F. 2001, in Astrophysics and Space Science Library 264, The Influence of Binaries on Stellar Population Studies, ed. D. Vanbeveren, 339 (astro-ph/0011248)
Zhu, X.-J., Howell, E. & Blair, D. 2010, MNRAS, 409, 132
Zwerger, T., & Mueller, E. 1997, A&A, 320, 209